14. Lombardi, J. R.; Klemperer, W.; Robin, M. B.; Basch, H.; Kuebler, N. A. *J. Chem. Phys.* **1969**, *51*, 33.
15. Hepburn, P. H.; Hollas, J. M. *J. Mol. Spectrosc.* **1974**, *50*, 126.
16. Vandersall, M.; Rice, S. A. *J. Chem. Phys.* **1983**, *79*, 4845.
17. (a) Sieber, H.; Riedle, E.; Neusser, H. *J. Chem. Phys. Lett.* **1990**, *169*, 191. (b) Sieber, H.; Bruno, A. E.; Neusser, H. J. *J. Phys. Chem.* **1990**, *94*, 203.
18. Modarelli, D. A.; Morgan, S.; Platz, M. S. *J. Am. Chem. Soc.* **1992**, *114*, 7034.
19. Modarelli, D. A.; Platz, M. S. *J. Am. Chem. Soc.* **1993**, *115*, 470.
20. Kim, T.-S.; Choi, Y. S.; Kwak, I. *J. Photochem. Photobiol. A.* **1997**, *108*, 123.
21. Kim, T.-S.; Kim, S. K.; Choi, Y. S.; Kwak, I. *J. Chem. Phys.* **1997**, *107*, 8719.
22. Schmitz, E.; Ohme, R. *Chem. Ber.* **1961**, *94*, 2166.
23. Frisch, M. J.; Trucks, G. W.; Schlegel, H. B.; Gill, P. M. W.; Johnson, B. G.; Robb, M. A.; Cheeseman, J. R.; Keith, T. A.; Petersson, G. A.; Montgomery, J. A.; Raghvachari, K.; Al-Laham, M. A.; Zakrzewski, V. G.; Oritiz, J. V.; Foresman, J. B.; Cioslowski, J.; Stefanov, B. B.; Nanayakkara, A.; Challacombe, M.; Peng, C. Y.; Ayala, P. Y.; Chen, W.; Wong, M. W.; Andres, J. L.; Replogle, E. S.; Gomperts, R.; Martin, R. L.; Fox, D. J.; Binkley, J. S.; Defrees, D. J.; Baker, J.; Stewart, J. P.; Head-Gordon, M.; Gonzalez, C.; Pople, J. A. *Gaussian 94*, Gaussian, Inc., Pittsburgh, PA, 1995.
24. Kim, T.-S.; Choi, Y. S. a low-resolution absorption spectrum of the gaseous dimethyldiazirine obtained with a UV-visible spectrometer, unpublished result.
25. Hout, R. F.; Levi, B. A.; Hehre, W. J. *J. Comput. Chem.* **1982**, *3*, 234.
26. Defrees, D. J.; McLean, A. D. *J. Chem. Phys.* **1985**, *82*, 333.
27. Pople, J. A.; Scott, A. P.; Wong, M. W.; Radom, L. *Isr. J. Chem.* **1993**, *33*, 345.

Molecular Dynamics Simulation for Bilayers of Alkyl Thiol Molecules at Solid-Solid Interfaces

Song Hi Lee*, Han Soo Kim†, and Hyungsuk Pak‡

Department of Chemistry, Kyungsung University, Pusan 608-736, Korea
†Department of Industrial Chemistry, Kangnung National University, Kangnung 212-702, Korea
‡Department of Chemistry, Seoul National University, Seoul 151-740, Korea
Received May 1, 1998

We present the results of molecular dynamics simulations for three different systems of bilayers of long-chain alkyl thiol [$S(CH_2)_{15}CH_3$] molecules on an solid-solid interface using the extended collapsed atom model for the chain-molecule. It is found that there exist two possible transitions: a continuous transition characterized by a change in molecular interaction between sites of different chain molecules with increasing area per molecule and a sudden transition from an ordered lattice-like state to a liquid-like state due to the lack of interactions between sites of chain molecules on different surfaces with increasing distance between two solid surfaces. The third system displays a smooth change in probability distribution characterized by the increment of *gauche* structure in the near-tail part of the chain with increasing area per molecule. The analyses of energetic results and chain conformation results demonstrate the characteristic change of chain structure of each system.

Introduction

In a previous paper,[1] we have performed several molecular dynamics (MD) simulations of monolayers of long-chain alkyl thiol[$S(CH_2)_{15}CH_3$] molecules on an air-solid interface using an extended collapsed atom model for the chain-molecule and a gold surface for the solid surface. We investigated the structure and thermodynamics of monolayers of long-chain alkyl thiol molecules on an air-solid interface as a function of area per molecule, especially, to study the phase transition in the monolayer, the fraction of trans formation, the thickness of the monolayer, monolayer tilting,Slattice defects, and diffusion of the chain-molecules. Also additional studies of how the area per molecule of the chain-molecule on the surface affects the characterization of Langmuir monolayer were carried out. The results from our MD simulations showed three possible transitions: a continuous transition characterized by a change in molecular configuration without changing in the lattice structure, a sudden transition characterized by the distinct lattice defects and perfect islands, and a third transition characterized by the appearance of a random, liquid-like state.

We have extended this study[1] to the bilayers of alkyl thiol molecules at a solid-solid interface. The bilayer of chain-molecules is very important for biological membranes,[2] because, in the bilayers, lipid-lipid interactions as well as lipid-intrinsic molecule (e.g., cholesterol and protein) interactions may be studied for a reasonably well-defined system. Also this study helps to understand the system of

Langmuir-Blodgett monolayers and multilayers,[3-5] surface adsorbed chain-molecules,[6,7] and molecular/liquid crystals of chain-molecules.[8,9]

In this study, we follow the MD simulation system of Biswas *et al.*[10] but extend our study to more complex systems. They fixed the heads of the chain-molecules on the surfaces, and kept the distance between two surfaces constant throughout the simulation. But this model showed neither the pseudohexagonal rotator phase phenomena nor the phase transition, since the head groups were fixed and the distance between two surfaces was fixed without changing the volume of the system. It is known that the dominant effect of the transition of the bilayer system is due to the longitudinal motion of the chains with an abundance of gauche defects at the interface. And we have considered the system in which each site of the head group interacts with the solid surface by a 12-3 Lennard-Jones[11,12] potential, leaving the orientation of the first bond with respect to the surface normal unrestricted.

The pseudohexagonal rotator phase in long-chain n-alkanes has been widely studied by experimentalists.[13-15] The results for the monolayer system obtained by us[1] displayed the pseudohexagonal rotator phase phenomena by the distinct lattice defects. This is due to the orientation of the first bond with respect to the surface normal was unrestricted. The results for the tilt angles calculated by Biswas *et al.*[10] showed the decrement of the chain tilt at higher temperature (350 K). The same results were observed in the monolayer systems studied by us.[1] The decrement of the chain tilt is due to the lattice isolation. Biswas *et al.*[10] calculated two tilt angles-local tilt and global tilt. The global tilt angles calculated in their work[10] included the effect of the azimuthal distribution of individual molecular tilt angles.

This paper is organized as follows. In Section II, details of the molecular model and molecular dynamics simulation method in a NVT ensemble are presented. We discuss our simulation results of monolayers of long-chain alkyl thiol molecules in the solid-solid interface in Section III and present the concluding remarks in Section IV.

Molecular Model and Molecular Dynamics Simulation Methods

Molecular Model. The systems studied in this work consist of 90 surfactant chain-molecules periodically replicated in the x- and y-directions. The heads of 45 chain-molecules are on the upper surface and the other 45 heads are on the lower surface. The initial configuration of those chain-molecules is treated not overlapped. The chain-molecules considered here consist of a sulfur head-group, 15 methylene segments, and a methyl tail-group. The molecular model used for the chain-molecules is so-called extended collapsed atom model, developed by Chynoweth *et al.*,[16] in which monomeric units (sulfur atom, methylene, or methyl) are typically treated as a single sphere (or site) with a Lennard-Jones (LJ) potential between the spheres. Not only sites on different chain-molecules but sites more than three apart on the same chain-molecule interact through a 12-6 LJ potential. C-C-C-C torsional rotation potential, introduced in Ryckaert and Bellemans' original collapsed atom model,[17] is also included.

The interaction between each site and the solid surface is given by a 12-3 LJ potential which have the form of[11,12]

$$V(z)=\frac{C_{12}}{(z-z_0)^{12}}-\frac{C_3}{(z-z_0)^3} \tag{1}$$

where z is the distance between each site and the surface, and C_{12}, C_3, and z_o are fitting potential parameters which are given in Table I for the several different sites.

Bond stretching interaction between adjacent sites on the same chain are also considered.[18] The potential energy associated with bond stretching between sites i and j is assumed to be harmonic and is given by

$$V_s=k_s(|\boldsymbol{r}_{ij}|-r_e)^2 \tag{2}$$

Here, $\boldsymbol{r}_{ij}$ is the bond vector, r_e is the equilibrium distance and k_s is the force constant (the last two are constant parameters depending upon the type of sites i and j only).

Bond angle bending denotes the interaction between three consecutively bonded sites i, j and k. The potential energy associated with bond angle bending is also harmonic and is given by

$$V_b(\theta)=k_b\,(\theta-\theta_o)^2 \tag{3}$$

where θ is C-C-C or S-C-C angle, θ_0 is the equilibrium bond angle, and k_b are the force constant (the last two are constant parameters depending upon the type of sites i, j and k only).

The changes in the equilibrium dihedral angles are subject to torsional rotational potential. Torsional rotation about a bond denotes the bonded interaction between four sites i, j, k and l. The potential energy associated with torsional rotation is represented by the original Ryckaert-Bellemans potential[17]

$$\begin{aligned}V_t(\psi)=a_0+a_1\cos(\psi)+a_2\cos^2(\psi)+a_3\cos^3(\psi)\\+a_4\cos^4(\psi)+a_5\cos^5(\psi)\end{aligned} \tag{4}$$

where ψ is the dihedral angle. The potential parameters - r_e, k_s, θ_0, k_b, a_0, a_1, a_2, a_3, a_4, and a_5 - used in our study are given in Table 1. The corresponding forces due to the potentials of Eqs. (2)-(4) are obtained by differentiation[19] with respect to the position vector of each site.

Molecular Dynamics Simulation in a Canonical Ensemble. In the present work, a canonical ensemble of fixed N (=90 chain-molecules), V (=volume of rectangular box), and T (=293.15 K) is chosen for the simulation ensemble. In this ensemble, three different systems of bilayers of chain-molecules are selected. The areas per molecule range from 15.40 to 51.77 Å^2/molecule and the distances between two solid surfaces are varied from 30.0 to 45.0 A. The preliminary molecular dynamics simulation of monolayer of the chain-molecules is started from a state at the area/molecule of 42.78 Å^2/molecule with the distance between two solid surfaces of 30.0 A. The lengths of the simulation box are X_L=44.73, Y_L=43.04, and fixed Z_L=30.0 A. The half of the head-group are on the lattice point of a regular hexagonal structure of the upper solid surface and the other half head-group are on the center of the hexagonal structure of the lower solid surface. In order to simulate smaller or larger area per molecule of monolayers, the box

Table 1. Potential parameters for $S(CH_2)_{15}CH_3$ molecule

Bond stretching	S-C	C-C	
r_e (nm)	0.182	0.153	
k_s (kJ/mol·nm^2)	132600	132600	
Bond angle bending	S-C-C	C-C-C	
θ_o (deg)	109.5	114.4	
k_b (kJ/mol·deg^2)	0.07915	0.07915	
L-J 12-6 potential	S	CH_2	CH_3
σ (nm)	0.425	0.3905	0.3905
ε (kJ/mol)	1.6629	0.4939	0.7325
L-J 12-3 potential	S	CH_2	CH_3
z_o (nm)	0.0269	0.086	0.086
C_{12} (10^7 kJ/mol)	3.3998	2.3280	2.8352
C_3 (kJ/mol)	1.5016	0.1422	0.1729

Torsional potential (kJ/mol)

a_1	a_2	a_3	a_4	a_5	a_6
9.279	12.156	-13.120	-3.060	26.240	-31.495

size is periodically increased or decreased in the x-, y-, and z-directions.

In this paper the simulation systems are three kinds: system A - bilayers of fixed distance between two solid surfaces (45.0 A) with areas per molecule ranging from 15.40 to 27.38 A^2/molecule, system B - bilayers of fixed area per molecule (42.78 A^2/molecule) with distances between solid surfaces ranging from 30.0 to 40.0 A, and system C - another bilayers of fixed distance between two solid surfaces (30.0 A) with areas per molecule ranging from 38.61 to 51.77 A^2/molecule. For the initial configurations of all the chain-molecules, the orientation of the first S-C bond with respect to the surface normal is unrestricted, the sulfur head group is located at the lattice point of a regular hexagonal structure, 2.4 A apart from the solid surface, and the consecutive methylene and methyl sites are placed in the z-direction so that the bond length and the bond angles are kept at 1.53 A and 109.5° respectively.

Gauss's principle of least constraint[20] is used to maintain the system at the constant temperature. The ordinary periodic boundary condition in the x- and y-directions only and minimum image convention for the LJ potential are applied with a spherical cut-off distance of radius 9.808 A. Gear's fifth order predictor-corrector method[21] is employed for time integration algorithm with time step of 0.5 fs (femto second). Each simulation is equilibrated for approximately 200,000 time steps (100 ps), and followed by 10,000 time steps (50 ps) for sampling. The trajectories (configurations and orientations) of the chain-molecules are stored every ten time steps (5 fs).

Results

Thermodynamics

Several potential energies calculated from our molecular dynamics simulations are given in Table 2. Lennard-Jones potential energies are almost monotonically increased with increasing area per molecule (fixed distance between two surfaces) except the smallest area per molecule case due to a large repulsion between chain-molecules and with increasing distance between two surfaces (fixed area per molecule), but chain-surface potential energies display the opposite trend. Dihedral energies are also increased with increasing area per molecule (fixed distance between two surfaces). C-C bond stretching and C-C-C bond angle bending energies display the same trend with small

Table 2. Average potential energies (kJ/mol) from our MD simulations for bilayer of $S(CH_2)_{15}CH_3$

Area/ molecule (A^2) -distance (A)	LJ potential energy	Chain-surface energy	Dihedral energy	C-C bond stretching energy	C-C-C bond angle bending energy
A 15.40-45.0	-74.8	-123.0	0.796	9.56	15.14
18.08-45.0	-126.9	-123.8	0.983	5.77	14.13
20.96-45.0	-120.5	-124.2	1.162	4.57	14.58
24.07-45.0	-115.9	-126.0	1.194	4.76	14.99
27.38-45.0	-109.6	-128.0	1.297	9.53	16.05
B 42.78-30.0	-97.3	-129.6	1.588	8.99	16.23
42.78-32.5	-90.2	-131.8	1.750	11.51	16.73
42.78-35.0	-81.3	-137.4	2.132	11.50	17.04
42.78-37.5	-80.4	-138.6	2.167	12.01	16.96
42.78-40.0	-79.8	-138.9	2.170	13.33	17.31
C 38.61-30.0	-98.5	-130.6	1.579	8.38	16.17
42.78-30.0	-97.3	-129.6	1.588	8.99	16.23
47.17-30.0	-94.4	-132.2	1.589	9.06	16.36
51.77-30.0	-92.4	-132.4	1.646	10.53	16.85

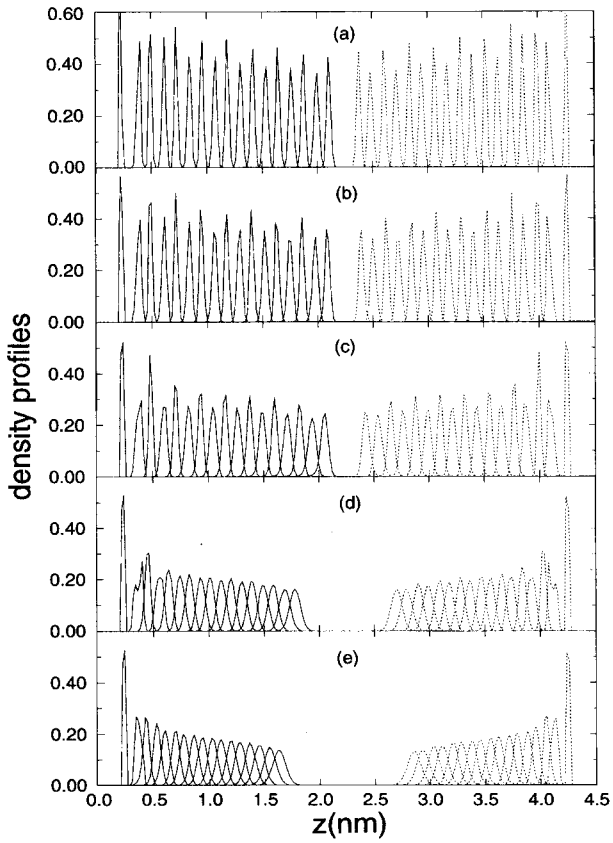

Figure 1. The density profiles of system A at five different areas per molecule: (a) 15.40, (b) 18.08, (c) 20.96, (d) 24.07, and (e) 27.38 A^2/molecule with the same distance between two solid surfaces of 45.0 A.

variance.

Structure

System A. This system is very similar to that studied by Biswas *et al.*[10] but the head group are not fixed on the surface in this study. In Figure 1, we show the probability distributions of segments normal to the surface for five different area per molecule ranging from 15.40 to 27.38 A^2/molecule with fixed distance of 45.0 A between two surfaces which are the primary measurers of local structure. The singlet probability $P_i(z)$ can be determined directly from our molecular dynamics simulations by $P_i(z)=<N_i(z)>/N$, where N is the total number of molecules, and $<N_i(z)>$ is the average over time of the number of segments i that are found in a slab of thickness Δz with distance z from the z=0 plane. Δz used in all simulations was equal to 0.2 A. The peaks are changed from the sharp non-overlapping to the broad overlapping as the area per molecule increases with fixed distance between two solid surfaces. In the smallest area per molecule, the repulsive interaction between sites of different chain molecules dominates and this makes all the chain molecules most upright. As the area per molecule increases, the interaction between sites of different chain molecules become attractive as seen in Table 2, and the system moves through energetically the most stable state in Figure 1(b), the appearance of overlapping of sites in Figure 1(c), and the broad overlapping in Figure 1(d) and (e). A clear transition between Figures 1(b) and 1(d) is observed with the intermediate state of Figure 1(c).

Chain conformation results from our molecular dynamics simulations for bilayers of $S(CH_2)_{15}CH_3$ are listed in Table 3. The values of head-to-tail distance, monolayer thickness, and trans bond fraction are plotted as a function of area per molecule in Figure 2. The head-to-tail distance is insensitive with the change of area per molecule. However, The monolayer thickness is directly related to the fraction of *trans* bond and decreases monotonically as the area per molecule is increased with a sudden decrease at 24.07 A^2/molecule. The behavior of non-changing head-to-tail

Table 3. Chain conformation results from our MD simulations for bilayer of $S(CH_2)_{15}CH_3$

Area/molecule (A^2)-distance (A)	Head-to-tail distance	Monolayer thickness	Trans bond fraction	Tilt angles		
				Eq.(5)	Eq.(6)	Eq.(7)
A 15.40-45.0	2.010	1.876	0.9997	22.24	21.04	13.00
18.08-45.0	2.004	1.863	0.9992	23.21	21.62	15.90
20.96-45.0	2.000	1.820	0.9928	26.10	24.50	21.10
24.07-45.0	1.993	1.547	0.9886	40.25	39.09	39.16
27.38-45.0	1.977	1.395	0.9702	46.50	45.13	44.54
B 42.78-30.0	1.878	1.779	0.9133	28.64	18.67	17.05
42.78-32.5	1.820	1.572	0.8722	39.14	30.26	27.26
42.78-35.0	1.691	1.120	0.7967	56.46	48.52	43.88
42.78-37.5	1.683	1.000	0.7883	60.44	53.55	44.97
42.78-40.0	1.637	0.971	0.7740	61.36	53.59	46.68
C 38.61-30.0	1.883	1.806	0.9161	27.00	16.44	15.63
42.78-30.0	1.878	1.779	0.9133	28.64	18.67	17.05
47.17-30.0	1.858	1.700	0.9084	32.98	23.76	21.10
51.77-30.0	1.856	1.662	0.9022	34.91	26.39	22.76

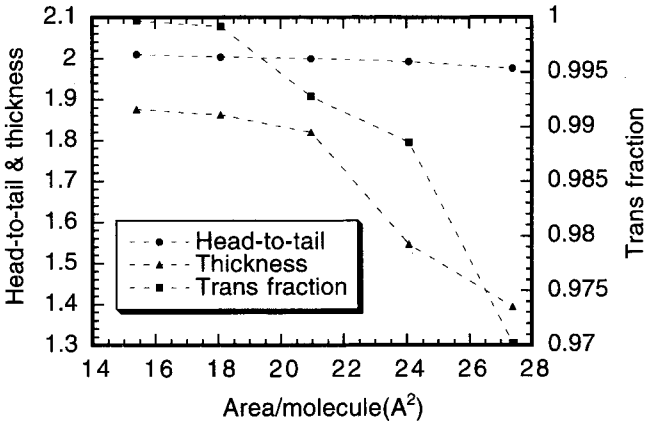

Figure 2. The head-to-tail distance, the monolayer thickness, and the fraction of trans bond of system A as a function of area per molecule with the same distance between two solid surfaces of 45.0 A.

distance with the large change of monolayer thickness indicates the significant tilting of the chain-molecules. As the monolayer thickness decreases with increasing area per molecule, the separation between tails of chain molecules adsorbed on the lower and upper surfaces is increased as seen in Figure 1 and the chain-surface energy is also increased due to more attractive interaction of chain molecules with the surface on which they adsorbed than with the other surface.

The tilt angle is sensitive to the change of the area per molecule. It is simply calculated from the monolayer thickness, l:

$$\cos = l/l_t, \tag{5}$$

where l_t is the thickness of a completely *trans* and upright monolayer. Or

$$\cos\theta = l/d, \tag{6}$$

with the head-to-tail distance, d. Another way to calculate the tilt angle is through the average of the tilt of all molecules

$$\cos\theta = \frac{1}{N}\sum_{i=1}^{i=N}\frac{\vec{u}_i\cdot\vec{u}_n}{|\vec{u}_i|\,|\vec{u}_n|} \tag{7}$$

where N is the total number of molecules, $\vec{u}_i$ is the vector that corresponds to the highest eigen value in the moment of inertia tensor, and $\vec{u}_n$ is the vector normal to the monolayer interface.

The tilt angles calculated from Eqs. (5), (6) and (7) as a function of area per molecule are shown in Figure 3. The three tilt angles show the same trend over all the areas per molecule with a sudden increase at 24.07 A^2/molecule and the comparison of these angles indicates that Eq. (5) overestimates the monolayer tilt with respect to Eq. (7) siince it assumes the absence of any gauche defects in the chain. That is why the behavior of the tilt angle from Eq. (5) is more similar to that of the monolayer thickness than Eq. (7). The tilt angle distribution changes significantly between 20.96 and 24.07 A^2/molecule which implies a kind of transition between them. This system with large distance between two solid surfaces shows similar behavior as that

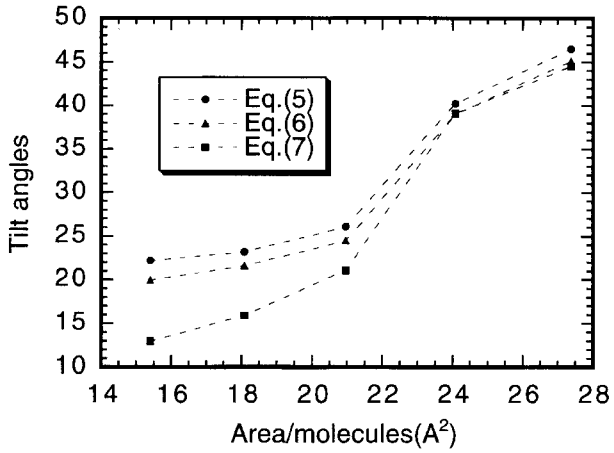

Figure 3. The tilt angles calculated from Eqs. (5), (6), and (7) of system A as a function of area per molecule with the same distance between two solid surfaces of 45.0 A.

of monolayer. In the MD study for substrate-supported monolayers of long-chain molecules by Bareman and Klein,[22] they reported very similar results that at the highest densities the chains align approximately normal to the substrate and show a continuous increase in the collective tilt as the molecular area is increased.

System B. This system is the reverse of system A in which bilayers of fixed area per molecule (42.78 A^2/molecule) with distances between solid surfaces range from 30.0 to 40.0 A. The density profiles of segments of this system are shown in Figure 4. The peaks are changed from the sharp overlapping to the non-structural broad overlapping as the distance between two solid surfaces increases with fixed area per molecule. In the shortest distance between two surfaces, the attractive interaction between sites of chain molecules on different surfaces makes the chain molecules upright, but segments are found most in their own sites and one lower sites of the upright configuration. It is worth noting that the tail group and upper segments are located at longer z-coordinates than in the case of system A. This is because of the strong attractive interaction between sites of chain molecules on different surfaces as when two combs are overlapped and because of the flexible property of the extended collapsed atom model for the chain molecule which results in the high C-C bond stretching and C-C-C bond angle bending energies in Table 2. As the distance between two surfaces increases, the interaction become less attractive due to less contact between sites of chain molecules on different surfaces, and the system moves through energetically the less stable state in Figure 4(b) and changes suddenly to a liquid-like state with the appearance of non-structural broad overlapping of sites in Figure 4(c), (d), and (e). In Figure 4(c), the chain molecules lose the support between them by a further backward of one surface and fall down on the surfaces. A clear phase transition between Figures 4(b) and 4(c) is observed.

The energetic change according to this phase transition from an ordered lattice-like state of Figure 4(b) to a liquid-like state of Figure 4(c) is clearly seen in the LJ potential, chain-surface, and dihedral energies of Table 2 but not in the C-C bond stretching and C-C-C bond angle bending

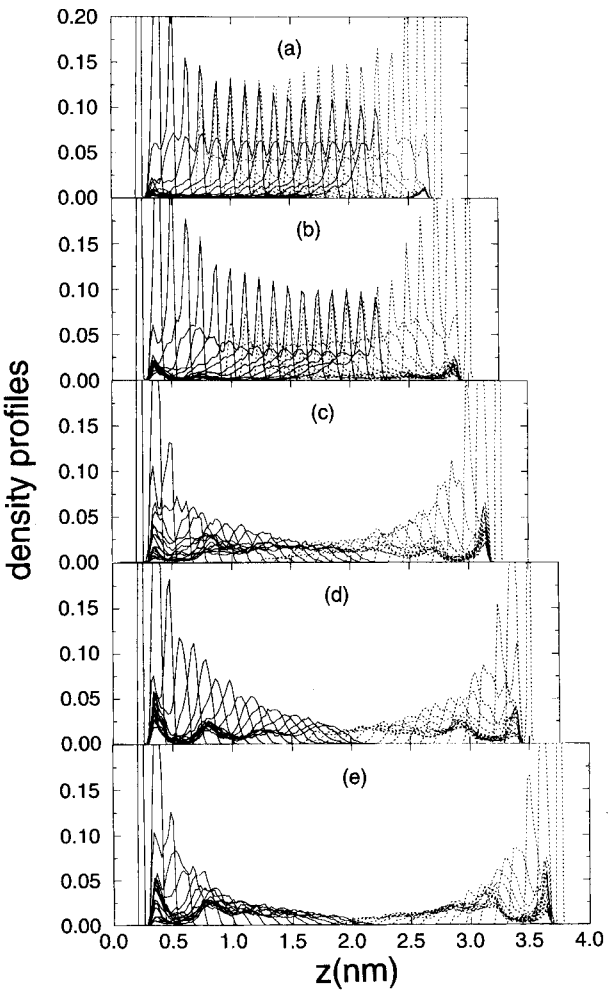

Figure 4. The density profiles of system B at five different distances between two solid surfaces: (a) 30.0, (b) 35.0, (c) 40.0, (d) 45.0, and (e) 50.0 A with the same area per molecule of 42.78 A^2/molecule.

energies.

The head-to-tail distance, monolayer thickness, and *trans* bond fraction of system B are plotted as a function of area

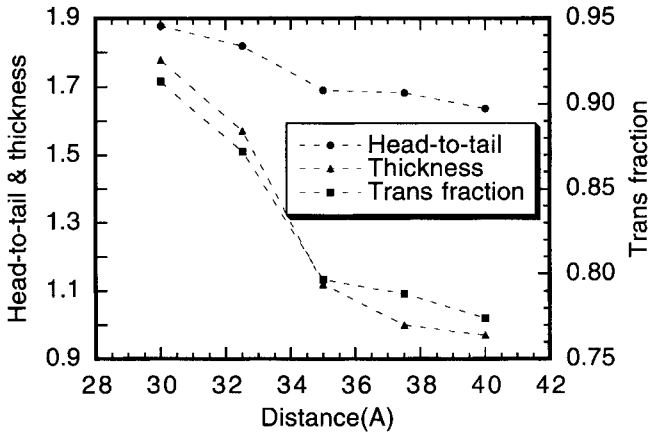

Figure 5. The head-to-tail distance, the monolayer thickness, and the fraction of trans bond of system B as a function of distance between two solid surfaces with the same area per molecule of 42.78 A^2/molecule.

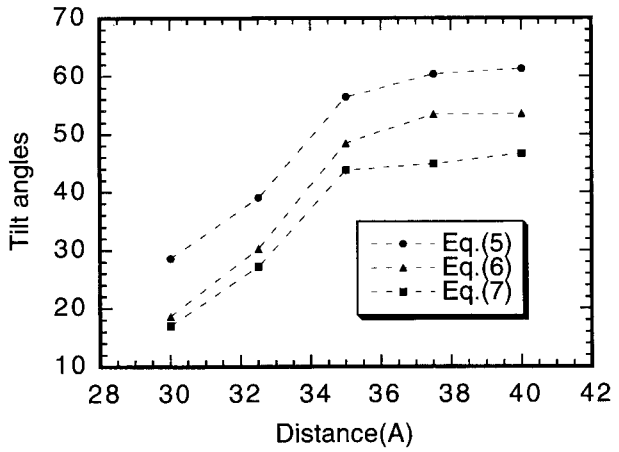

Figure 6. The tilt angles calculated from Eqs.(5), (6), and (7) of system B as a function of distance between two solid surfaces with the same area per molecule of 42.78 A^2/molecule.

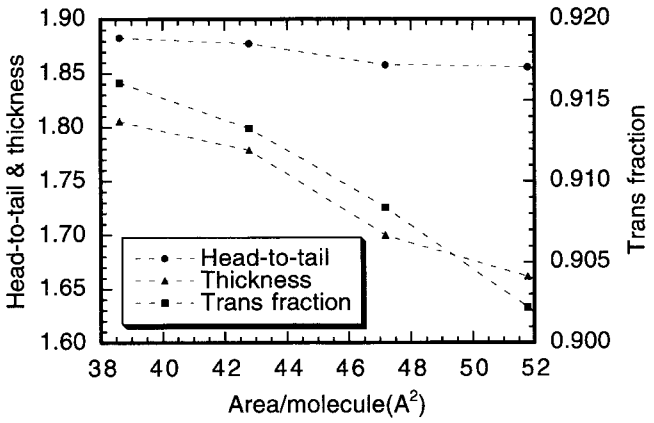

Figure 8. The head-to-tail distance, the monolayer thickness, and the fraction of trans bond of system C as a function of area per molecule with the same distance between two solid surfaces of 30.0 A.

per molecule in Figure 5. These three properties show a sudden change of the system from 32.5 to 35.0 A^2/molecule. The low values of head-to-tail distance at 35.0, 37.5, and 40.0 A^2/molecule indicate a large amount of gauche defects in the chains which can be seen in the *trans* fraction. The same trend of monolayer thickness at those areas per molecule result in the high tilt angles as seen in Figure 6. The tilt angles of system B calculated from Eqs. (5), (6) and (7) as a function of distance between two surfaces also show a sudden change of the system from 32.5 to 35.0 A^2/molecule.

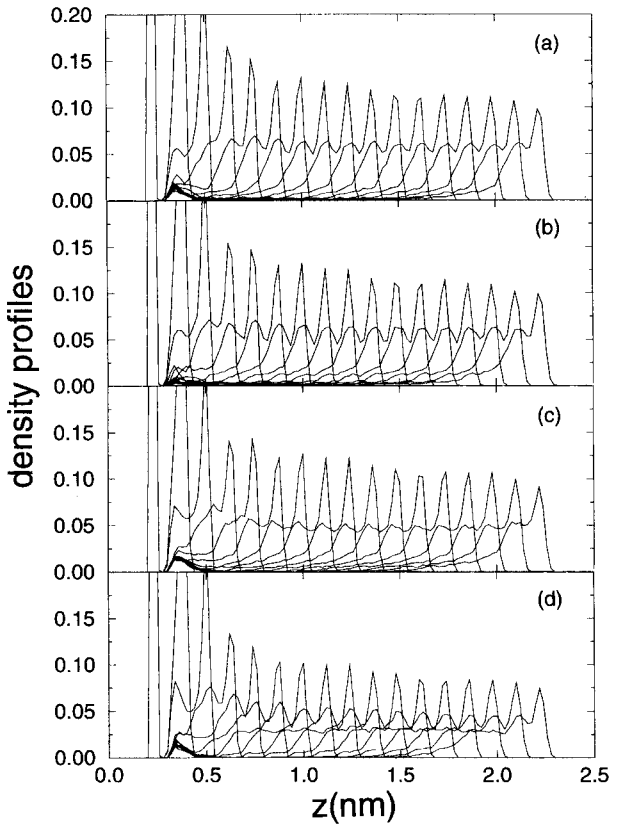

Figure 7. The density profiles of system C at four different areas per molecule: (a) 38.61, (b) 42.78, (c) 47.17, and (d) 51.77 A^2/molecule with the same distance between two solid surfaces of 30.0 A. The density profiles for only the monolayer are shown. See the text.

System C. This system is similar to system A but bilayers of fixed distance between two solid surfaces (30.0 A) with areas per molecule range from 38.61 to 51.77 A^2/molecule. The fixed distance between two surfaces is decreased while the areas per molecule are increased due to the interaction between sites of chain molecules on different surfaces when compared with system A. The density profiles of segments for only the monolayer of this system are shown in Figure 7 for simplicity. The density profiles for the other monolayer can be created by the mirror reflection of these density profiles at z=1.5 nm. For example, the result by the mirror reflection of Figure 7(b) is Figure 4(a). The density profiles and chain conformation results in Figures 8 and 9 calculated in this system are completely different from those in system A.

There is no sudden change in the density profiles, head-to-tail distance, monolayer thickness, *trans* fraction, and tilt angles as the area per molecule increases with fixed distance between two solid surfaces. A smooth change in probability distribution is characterized by the increment of gauche structure in the near-tail part. However, if the distance between two surfaces of MD simulation is extended far beyond 51.77 A^2/molecule, a different type of density profile is expected from the change in the positions of segments from Figure 7(c) to (d). For example, the tail group is found most in its own site and one lower site of the upright configuration in Figure 7(c) but in its own site and up to three lower sites of the upright configuration in Figure 7(d).

Finally, we have shown the fraction of *trans* bond of five different systems of area per molecule-distance between two solid surfaces in Figure 10. First, the decrease of the *trans* fraction towards the tail group could be attributed to the free motion of the tail group. Generally speaking, gauche defects are more likely found in the lower part of the chain while trans bonds in the upper part. This result is rather different from that of Biswas *et al.*[10] in which the middle of the chain had the highest extent of order. The difference comes mainly from the fixity of the head group on the

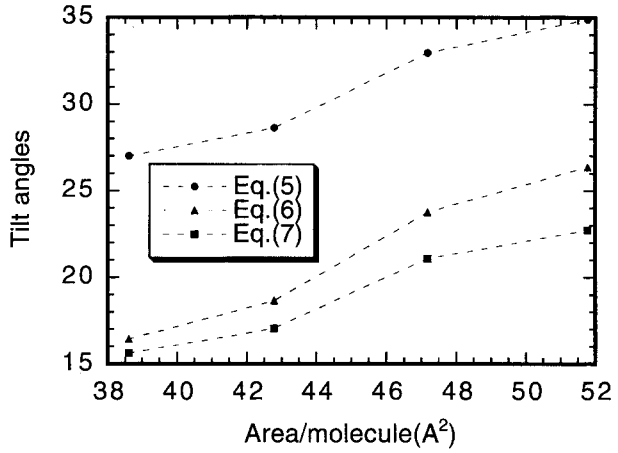

Figure 9. The tilt angles calculated from Eqs. (5), (6), and (7) of system C as a function of area per molecule with the same distance between two solid surfaces of 30.0 A.

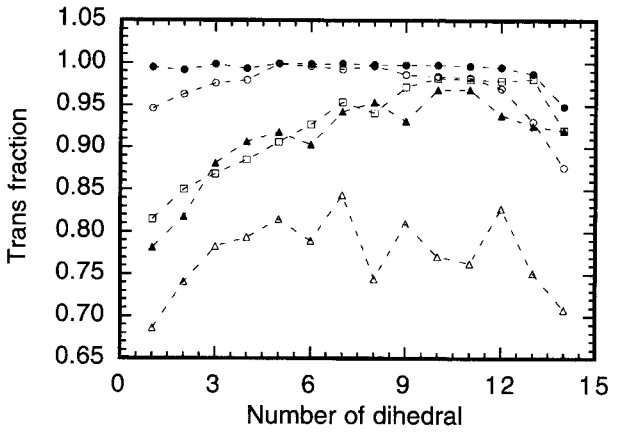

Figure 10. The fraction of *trans* bond of five different systems of area per molecule-distance between two solid surfaces: 20.96-45.0 (●), 27.38-45.0 (○), 42.78-30.0 (□), 42.78-40.0 (△), and 51.77-30.0 (▲).

surfaces. However, the first two bilayers of 20.96-45.0 and 27.38-45.0 (system A) have the same trend as Biswas *et al.*[10] because system A has almost the same area per molecule and distance between two surfaces as that of Biswas *et al.*[10] even though the head group are not fixed in this study.

The change in *trans* bond fraction from 20.96-45.0 (Figure 1(c)) to 27.38-45.0 (Figure 1(e)) is very small even though a clear transition is predicted in system A. On the other hand, the change from 42.78-30.0 (Figure 4(a)) to 42.78-40.0 (Figure 4(d)) is remarkable which reflects the phase transition from the ordered lattice-like state to the liquid-like state in system B. The small change in *trans* bond fraction is also observed from 42.78-30.0 to 51.77-30.0 in system C.

Concluding Remarks

We present the results of molecular dynamics simulations of bilayers of long-chain alkyl thiol $[S(CH_2)_{15}CH_3]$ molecules on an solid-solid interface using the extended collapsed atom model for the chain-molecule. Several molecular dynamics simulations have been performed on three different systems-bilayers of fixed distance between two solid surfaces (45.0 A) with areas per molecule ranging from 15.40 to 27.38 A^2/molecule (system A), bilayers of fixed area per molecule (42.78 A^2/molecule) with distances between solid surfaces ranging from 30.0 to 50.0 A (system B), and another bilayers of fixed distance between two solid surfaces (30.0 A) with areas per molecule ranging from 38.61 to 51.77 A^2/molecule (system C). It is found that there exist two possible transitions: a continuous transition characterized by a change in molecular interaction between sites of different chain molecules in system A and a sudden transition from an ordered lattice-like state to a liquid-like state due to the lack of interactions between sites of chain molecules on different surfaces in system B. System C displays a smooth change in probability distribution characterized by the increment of gauche structure in the near-tail part of the chain. The analyses of energetic results and chain conformation results such as head-to-tail distance, monolayer thickness, and trans bond fraction demonstrate the characteristic change of chain structure of each system.

Acknowledgment. This work was supported by Basic Science Research Institute Program, Ministry of Education (BSRI-96-3414). S. H. L. thanks the Korea Institute of Sciences and Technology for access to its Cray-C90 super computer and the Tongmyung University of Information Technology for access to its IBM SP/2 computers.

References

1. Lee, S. H.; Kim, H. S. *Bull. Korean Chem. Soc.* **1996**, *17*, 700.
2. Seeling, J.; Seeling, A. *Q. Rev. Biophys.* **1980**, *13*, 19.
3. Northrup, S. H.; Curvin, S. *J. Phys. Chem.* **1985**, *89*, 4707.
4. Khalatur, P. G.; Pavlov, A. S.; Balabaev, N. K. *Macromol. Chem.* **1987**, *188*, 3029.
5. Poster, R. W.; Venable, R. M.; Karplus, M. *J. Chem. Phys.* **1988**, *89*, 1112.
6. Milik, M.; Kolinski, A; Skolnick, J. *J. Chem. Phys.* **1990**, *93*, 4440.
7. Croxton, C. A. *J. Phys.* **1986**, *A19*, 987.
8. Bareman, J. P.; Cardini, C.; Klein, M. L. *Phys. Rev. Lett.* **1988**, *60*, 2152.
9. Kox, A. J.; Michels, J. P. J.; Wiegel, F. W. *Nature* **1980**, *287*, 317.
10. Biswas, A.; Schurman, B. L. *J. Chem. Phys.* **1991**, *95*, 5377.
11. Hautman, J.; Klein, M. L. *J. Chem. Phys.* **1989**, *91*, 4994.
12. Hautman, J.: Klein, M. L. *J. Chem. Phys.* **1990**, *93*, 7483.
13. Maroncelli, M.; Chi, S. P.; Strauss, H. L.; Snyder, R. G. *J. Am. Chem. Soc.* **1982**, *104*, 6237.
14. Doucet, J.; Denicolo, J.; Craievich, A. *J. Chem. Phys.* **1981**, *75*, 1523.
15. Barnes, J. D. *J. Chem. Phys.* **1973**, *58*, 5193.
16. Chynoweth, S.; Klomp, U. C.; Michopoulos Y. *J. Chem. Phys.* **1991**, *95*, 3024.
17. Ryckaert, J.-P.; Bellemans, A. *Faraday Discuss. Chem. Soc.* **1978**, *66*, 95.
18. van der Ploeg, P.; Berendsen, H. J. C. *Mol. Phys.* **1983**, *49*, 233.
19. Chynoweth, S.; Klomp, U. C.; Scales, L. E. *Comput. Phys. Commun.* **1991**, *62*, 297.

20. (a) Evans, D. J.; Hoover, W. G.; Failor, B. H.; Moran, B.; Ladd, A. J. C. *Phys. Rev.* **1988**, A. *28*, 1016. (b) Simmons, A. D.; Cummings, P. T. *Chem. Phys. Lett.* **1986**, *129*, 92.
21. Gear, W. C. *Numerical Initial Value Problems in Ordinary Differential Equations*; McGraw-Hill, New York, 1965.
22. Bareman, J. P.; Klein, M. L. *J. Phys. Chem.* **1990**, *94*, 5202.

Fluorescence and Laser Light Scattering Studies of Modified Poly(ethylene-*co*-methylacrylate) Ionomers on the Formation of Stable Colloidal Nanoparticles in Aqueous Solution

Sang-Ihn Yeo and Kyu Whan Woo*

Department of Chemistry Education, Seoul National University, Seoul 151-742, Korea
Received May 1, 1998

Fluorescence and dynamic light scattering measurements were applied to the study of formation and structure of aggregated colloidal particles in modified poly(ethylene-*co*-methylacrylate) ionomers in aqueous solution. Both 8-anillino-1-naphthalene-sulfonic acid (ANS) and pyrene were used as fluorescence probe to obtain the information on the structure of particle surface and inside, respectively. Three different ionomers used in this study started to aggregate at very dilute concentration, $3\text{-}8\times10^{-6}$ g/mL. In this study, we demonstrate that the polyethylene ionomers can form stable nanoparticles. The hydrophobic core made of the polyethylene backbone chains is stabilized by the ionic groups on the particle surface. Such a formed stable nanoparticles have a relatively narrow size distribution with an average radius in the range of 27-48 nm, depending on the kind of ionic groups. Once the stable particles are formed, the particle size distributions were nearly constant. This study shows another way to prepare surfactant-free polyethylene nanoparticles.

Introduction

Currently the term ionomer applies to a much larger category of polymers that is made up primarily of non-polar repeating units, with a small percentage of salt-containing units.[1-2] Most common non-polar comonomers used are ethylene and styrene. More than 30 years after the introduction of Surlyn® by DuPont, an intense research effort has been devoted to ionomers. Recently for environment reasons, attention has been focused on polymers that can be used in water-based formulations. The association/dissociation of ionomers in nonpolar and polar solvents have been a focused issue for more than 10 years, and the lightly sulfonated polystyrene ionomer was usually chosen as a model compound.[3] In nonpolar solvent, such as tetrahydrofuran (THF) and xylene, the ionic groups are not completely dissociated, but exist as solvated ion-pairs. Consequently these lead to the association of ionomers, which has been experimentally confirmed by rheology, light scattering, small angle neutron scattering and fluorescence.[4-10] When dissolving in a polar solvent, all phenomena related to the aggregation in nonpolar solvents disappear because of the dissociation of the ion-pairs. On the other hand, the study of the ionomers in aqueous media has attracted much less attention because of the poor solubility of its hydrophobic backbone in water. Recently, it has been found that randomly carboxylated and lightly sulfonated polystyrene ionomer chains can form stable colloidal nanoparticles in water if a dilute solution of an ionomer in tetrahydrofuran (THF) is added dropwise into an excessive amount of water.[11] Kutsumizu *et al.*[12] investigated the aggregate-water interface and the local mobility of aggregate inside.

In the present work, fluorescence together with laser light scattering were used to demonstrate that the polyethylene ionomers in which the ionic groups such as acrylate potassium salt, acrylamide, acrylic acid are introduced can form stable colloidal nanoparticles in water. The emphasis of this study will be on how the formation and structure of the stable nanoparticles depends on the kind of ionic groups.

Experimental Section

Modification of PE-7.6MA. The modification of poly(ethylene-*co*-methylacrylate) (PE-7.6MA), which contains 7.6 mol % methylacrylate, is carried out as described previously.[13] The weight-average molecular weight (M_w) and the number-average molecular weight (M_n) of PE-7.6MA were obtained from (GPC) (see Table 1). The mole fractions of the pendant ionic groups were calculated based on nitrogen analysis and the KOH amounts used in hydrolysis. Three modified ionomer samples were used in this study. The kind and content of the pendant ionic groups of these three samples are as follows: One of them [poly(ethylene-*co*-acrylate potassium salt)] contains 7.6 mol% acrylate potassium salts (designated as PE-7.6KAA hereafter). Another ionomer sample [poly(ethylene-*co*-acrylate potassium salt-*co*-acrylamide)] contains 3.8 mol% acrylate potassium salts and 3.8 mol% amide groups